

Secondary structures and functional requirements for thiM riboswitches from *Desulfovibrio vulgaris*, *Erwinia carotovora* and *Rhodobacter spheroides*

Andrea Rentmeister^a, Günter Mayer^a, Nicole Kuhn and Michael Famulok*

LIMES-Institute, Program Unit Chemical Biology and Medicinal Chemistry, c/o Kekulé-Institute for Organic Chemistry and Biochemistry of the University of Bonn, Gerhard-Domagk-Straße 1, D-53121 Bonn, Germany

*Corresponding author
e-mail: m.famulok@uni-bonn.de

Abstract

Bacterial thiM riboswitches contain aptamer domains that bind the metabolite thiamine pyrophosphate (TPP). Binding of TPP to the aptamer domain induces structural rearrangements that are relayed to the expression domain, thereby interfering with gene expression. Here, we report identification of three putative thiM riboswitches from different bacteria and analysis of their secondary structures. Chemical probing revealed that the riboswitches share similar secondary structures in their aptamer domains that can communicate with the highly variant expression domains in a mechanism likely involving sequestration of the Shine-Dalgarno sequence. Remarkably, the aptamer domain of the thiM gene of *Desulfovibrio vulgaris* binds TPP with similar affinity and selectivity as that of *Escherichia coli*, although nucleotides previously shown to form direct contacts to the metabolite are mutated. We also designed small RNA hairpins for each riboswitch that bind the RNA only in the absence of the metabolite. Our study shows that aptamer domains in riboswitches with high similarity in their secondary structures can communicate with a broad variety of non-related expression domains by similar mechanisms.

Keywords: chemical probing; *Desulfovibrio vulgaris*; *Erwinia carotovora*; hairpin; *Rhodobacter spheroides*; riboswitch; thiamine pyrophosphate; thiM.

Introduction

Riboswitches are a class of recently identified regulatory RNAs located in the untranslated regions of metabolic genes (Kubodera et al., 2003; Winkler and Breaker, 2003, 2005; Noeske et al., 2005; Nudler, 2006). They contain an aptamer domain that serves as a regulatory element that binds metabolites and biological cofactors, such as

thiamine pyrophosphate (TPP) (Winkler et al., 2004; Noeske et al., 2006), vitamin B₁₂ (Nahvi et al., 2004; Borovok et al., 2006; Sudarsan et al., 2006), S-adenosylmethionine (Winkler et al., 2003; Corbino et al., 2005; Fuchs et al., 2006; Montange and Batey, 2006; Sudarsan et al., 2006), amino acids (Sudarsan et al., 2003b; Mandal et al., 2004) and purine derivatives (Batey et al., 2004; Mandal and Breaker, 2004; Serganov et al., 2004; Noeske et al., 2007). Binding within the aptamer domain occurs in an adaptive binding mechanism which allows transducing conformational changes to a regulatory domain, often referred to as expression domain, which then negatively or positively regulates gene expression via different mechanisms. These include transcription termination, inhibition of translation initiation as well as alternative splicing.

One of the most widespread classes of riboswitches known to date are TPP-binding riboswitches which have been found in all three domains of life (Miranda-Rios et al., 2001; Rodionov et al., 2002; Winkler et al., 2002; Kubodera et al., 2003; Sudarsan et al., 2003a; Henkin and Grundy, 2006; Miranda-Rios, 2007). Located upstream of several *thi* genes, examples of TPP-binding riboswitches have been found for all three known mechanisms. The thiM riboswitch is located in the 5'-untranslated region (UTR) of the *thiM* gene, which codes for the hydroxyethylthiazole kinase (HET) and regulates gene expression on the level of translation initiation. The representative from *Escherichia coli* has been thoroughly characterized, both structurally (Serganov et al., 2006; Thore et al., 2006) and biochemically (Winkler et al., 2002; Yamauchi et al., 2005; Edwards and Ferre-D'Amare, 2006; Rentmeister et al., 2007). Crystallographic data of the aptamer domains of thiM riboswitches have shown that in the presence of TPP the aptamer domain forms a binding pocket consisting of two parallel helices grabbing the ligand from both ends (Edwards and Ferre-D'Amare, 2006; Serganov et al., 2006; Thore et al., 2006). TPP is located perpendicular to these helices and the negative charges of its pyrophosphate moiety are overcome by complexation of two Mg²⁺ ions (Edwards and Ferre-D'Amare, 2006; Serganov et al., 2006). In the presence of TPP, the expression domain forms a hairpin with a long stem which is formed by sequestration of the Shine-Dalgarno (SD) sequence (Winkler et al., 2002; Serganov et al., 2006). Thus, in the presence of TPP, the SD sequence is not available for binding to the ribosome and translation initiation is inhibited. Recent studies, largely based on chemical and enzymatic probing of the entire thiM riboswitch from *E. coli*, revealed that in the absence of TPP the RNA adopts a different structure in which only parts of the ligand-binding pocket are pre-

^aThese authors contributed equally to this work.

formed, whereas parts of the aptamer domain base pair with parts of the expression domain (Rentmeister et al., 2007). The SD sequence and nucleotides located downstream thereof are not involved in base pairing at all, supporting a mechanism that involves sequestration of the SD in the presence of TPP.

Owing to the importance and prevalence of TPP-binding riboswitches, we sought to characterize their representatives in other bacteria with respect to their secondary structures, binding properties and gene regulation mechanisms. ThiM genes in many bacteria contain riboswitches regulated by TPP (Rodionov et al., 2002). There appears to be a tight phylogenetic relationship between the aptamer domains of thiM riboswitches from different organisms. Most of the genes containing TPP-regulated riboswitches show considerable homologies in their TPP-binding domains, which greatly facilitates their identification. In contrast, the phylogenetic conservation between the related expression domains is considerably less pronounced. Thus, the mode of metabolite binding is probably highly similar within different TPP-binding riboswitches. However, it remains unclear how riboswitches use highly variable sequences in their expression domains to perform the same task – in the case of thiM inhibition of translation initiation. Therefore, we analyzed riboswitches from other bacteria to find out if similar rearrangements to the ones known from *E. coli* thiM occur in other thiM riboswitches, despite their barely conserved expression domain.

Results

Discovery of thiM riboswitches in other organisms by phylogenetic comparison

By analyzing phylogenetic relationships of the 5'-UTRs of thiM genes in bacteria other than *E. coli*, we found thiM riboswitches in *Erwinia carotovora* (ERC), *Rhodobacter spheroides* (RS) and *Desulfovibrio vulgaris* (DV), respectively, which have not been characterized up to now. Our analysis included only thiM riboswitches that (i) directly regulate the expression of HET, (ii) function by SD sequestration as opposed to transcriptional regulation (recognized by the lack of poly-U stretches in the 5'-vicinity of the SD sequence), (iii) share a clearly identifiable aptamer domain, and (iv) diverge from one another by more than 1–4 mutations. As expected, these riboswitches are highly conserved in their aptamer domains, whereas the expression domains show no similarities in their primary sequences (Figure 1A). Figure 1B–E compares sequence and secondary structure of the aptamer domains of the three riboswitches with the conserved structure of the proposed THI-element (Rodionov et al., 2002).

Conserved nucleotides within the aptamer domains of the ERC (Figure 1D) and RS (Figure 1E) riboswitches are in almost perfect agreement with the THI-element proposed by Rodionov et al. (2002) (highlighted nucleotides are in bold font). Out of the invariant positions within the

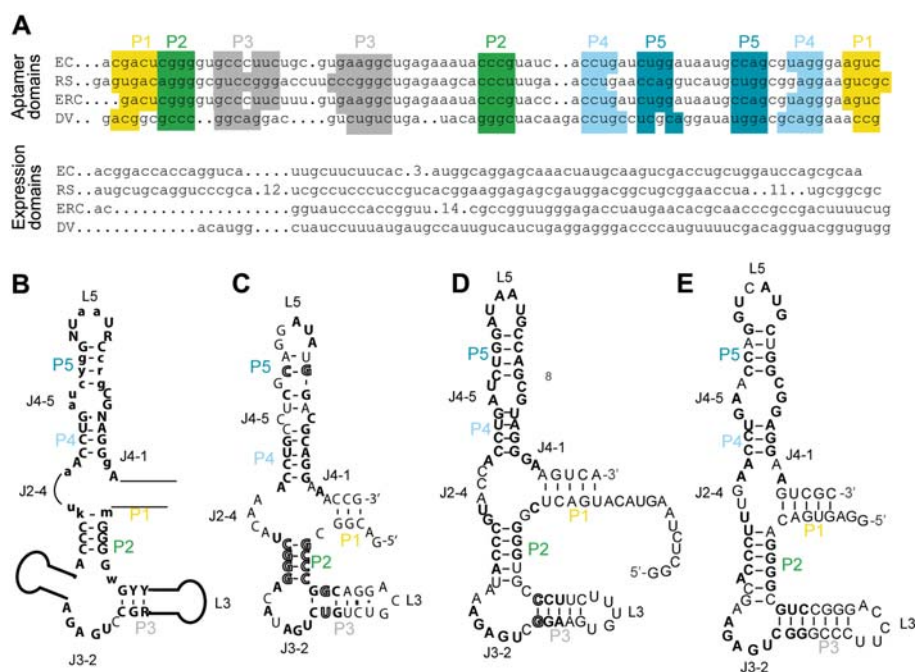


Figure 1 Conserved putative secondary structures of the aptamer domains of thiM riboswitches from different bacteria.

(A) Phylogenetic comparison of thiM riboswitches. Sequences of the aptamer domains of riboswitches found in the 5'-UTR of thiM genes in *E. coli*, *D. vulgaris*, *E. carotovora* and *R. spheroides*. Boxed nucleotides indicate the thi-box sequences that are characteristic to all TPP regulated genes. Sequences of the expression domains of riboswitches found in the 5'-UTR of thiM genes in different bacteria. The sequences are continuous between aptamer and expression domain. (B) The conserved structure of the THI-elements as described by Rodionov et al. (2002). Capital letters indicate invariant positions. Lowercase letters indicate strongly conserved positions. Degenerate positions are as follows: R, A or G; Y, C or U; K, G or U; M, A or C; N, any nucleotide. (C) Putative secondary structures of the aptamer domain of thiM riboswitches from *D. vulgaris*. Conserved nucleotides of the THI-elements are indicated by letters in bold font. Conserved but inverted base pairs are indicated by white letters framed in black. (D) Putative secondary structures of the aptamer domain of thiM riboswitches from *E. carotovora*. (E) Putative secondary structures of the aptamer domain of thiM riboswitches from *R. spheroides*.

THI-element, only stem P3 of ERC shows an inverted C/G base pair instead of G/C. In addition, ERC perfectly agrees with all of the strongly conserved positions of the THI-element. Within the conserved positions, RS shows four deviations from the THI-element: a U/A mutation in J4-5, an A-U base pair instead of a G-C base pair within stem P5, an A/C mutation in loop L5 and a G/A mutation within J4-1. None of these nucleotides have been shown to be important or even essential for interaction with TPP, according to the crystal structures (Edwards and Ferre-D'Amare, 2006; Serganov et al., 2006).

The aptamer domain of the DV thiM riboswitch (Figure 1C), however, exhibits several deviations from the conserved structure of the THI-element: several of the invariant positions within the THI-element are not conserved in the DV riboswitch. The entire stem P2 as well as the Y-G base pair within stem P3 are conserved, but inverted with respect to the THI-element. Furthermore, stem P5 exists, but does not resemble the THI-element except for the C-G base pair adjacent to J4-5. Within loop L5, only two A nucleotides and one U nucleotide are in agreement with the THI-element. However, stem P4 is conserved.

Most importantly, the single stranded UGAGA motif within J3-2, which was termed invariant by Rodionov et al. (2002), is mutated in DV to form a UGAUA motif. In crystal structures of its *E. coli* counterpart, this motif (and notably the G which is mutated to U in DV) has been shown to interact directly with the 4-amino-5-hydroxymethyl-2-methylpyrimidine (HMP) moiety of the ligand TPP in stacking interactions. Thus, the sequence in the 5'-UTR of the thiM gene in *D. vulgaris* exhibited such a considerable degree of deviation in the aptamer domain as compared to those from the *E. coli*, *E. carotovora* and *R. spheroides* that we considered it necessary to verify the ability of the putative DV aptamer domain to bind to TPP.

The 5'-UTR of *D. vulgaris* binds to TPP but not thiamine

To investigate whether the putative thiM riboswitch from *D. vulgaris* is indeed capable of binding to TPP, we performed binding studies by isothermal titration calorimetry (ITC) (Figure 2). We determined a dissociation constant of 232 nM for the DV riboswitch/TPP interaction, which is comparable to the K_d of 200 nM determined analogously with the thiM riboswitch from *E. coli* (Mayer et al., 2007). No binding could be observed for thiamine (Figure 2, gray diamonds). These data verify that the 5'-UTR of the thiM gene in *D. vulgaris* contains a TPP-binding domain which is, like other TPP-binding domains in various riboswitches, able to distinguish between TPP and the closely related analog thiamine.

Chemical probing of thiM riboswitches from *D. vulgaris*, *E. carotovora* and *R. spheroides*

We have previously analyzed the TPP-free form of the full-length thiM riboswitch from *E. coli* and found that the aptamer domain is only partially pre-formed in the absence of TPP. Therefore, we now sought to analyze the secondary structures of the full-length thiM riboswitches from *D. vulgaris*, *E. carotovora* and *R. spheroides* in the

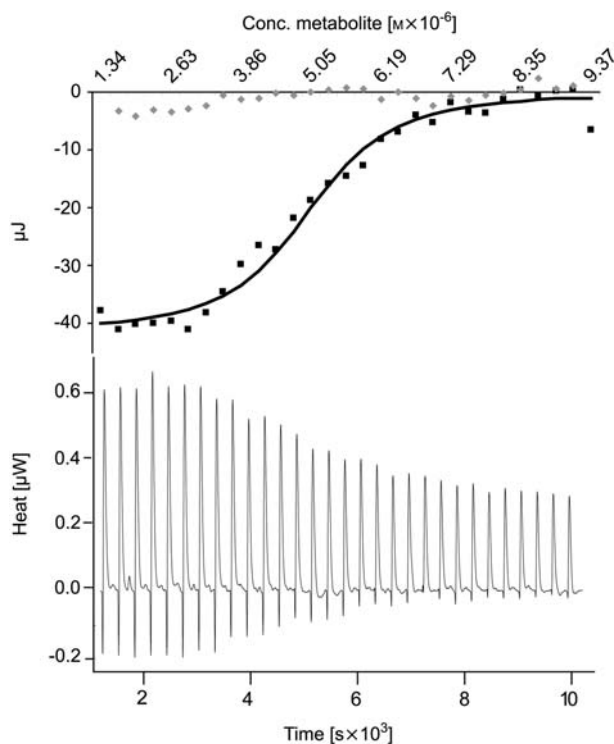


Figure 2 Affinity determination of the thiM riboswitch from *D. vulgaris*.

Isothermal titration calorimetry was used to determine binding of TPP (black squares and fitted line) and thiamine (gray diamonds), respectively, to *D. vulgaris* thiM. The titration curve is shown in the lower panel and resulting data are depicted as binding curve in the upper panel.

absence of TPP. The results of chemical probing as well as derived secondary structures are depicted in Figure 3.

Chemical probing of thiM riboswitch from *D. vulgaris*

The aptamer domain of the proposed DV riboswitch adopts the secondary structure expected from conserved structure of the THI-element. The predicted stems P1–P5 are confirmed by chemical probing (Figure 3A). Chemical probing shows modifications for the single-stranded regions J3-2, J2-4, L5 and J4-1 within the aptamer domain. This result confirms that the secondary structure of the aptamer domain fulfills the structural requirements of the THI-element. In contrast to the full-length thiM riboswitch from *E. coli*, however, the aptamer domain of full-length DV seems to be entirely pre-formed even in the absence of TPP.

The expression domain is able to form a hairpin loop L8 with adjacent stems P8, P7 and P6. The resolution of chemical probing is limited to nt116 due to overlapping primer-binding sites needed for reverse transcription. Therefore, we can only assume that the SD sequence will be single stranded in the absence of TPP. Chemical probing shows intense modifications for U94, U95 and U97 comprising bulge J7-8 as well as for nucleotides <nt110 which belong to loop L8 and the putative stem P8. From these data, we conclude that in the thiM RNA of *D. vulgaris*, stem P8 is only loosely pre-formed in the absence of TPP.

We also performed chemical probing with four different concentrations of kethoxal, a chemical probe that select-

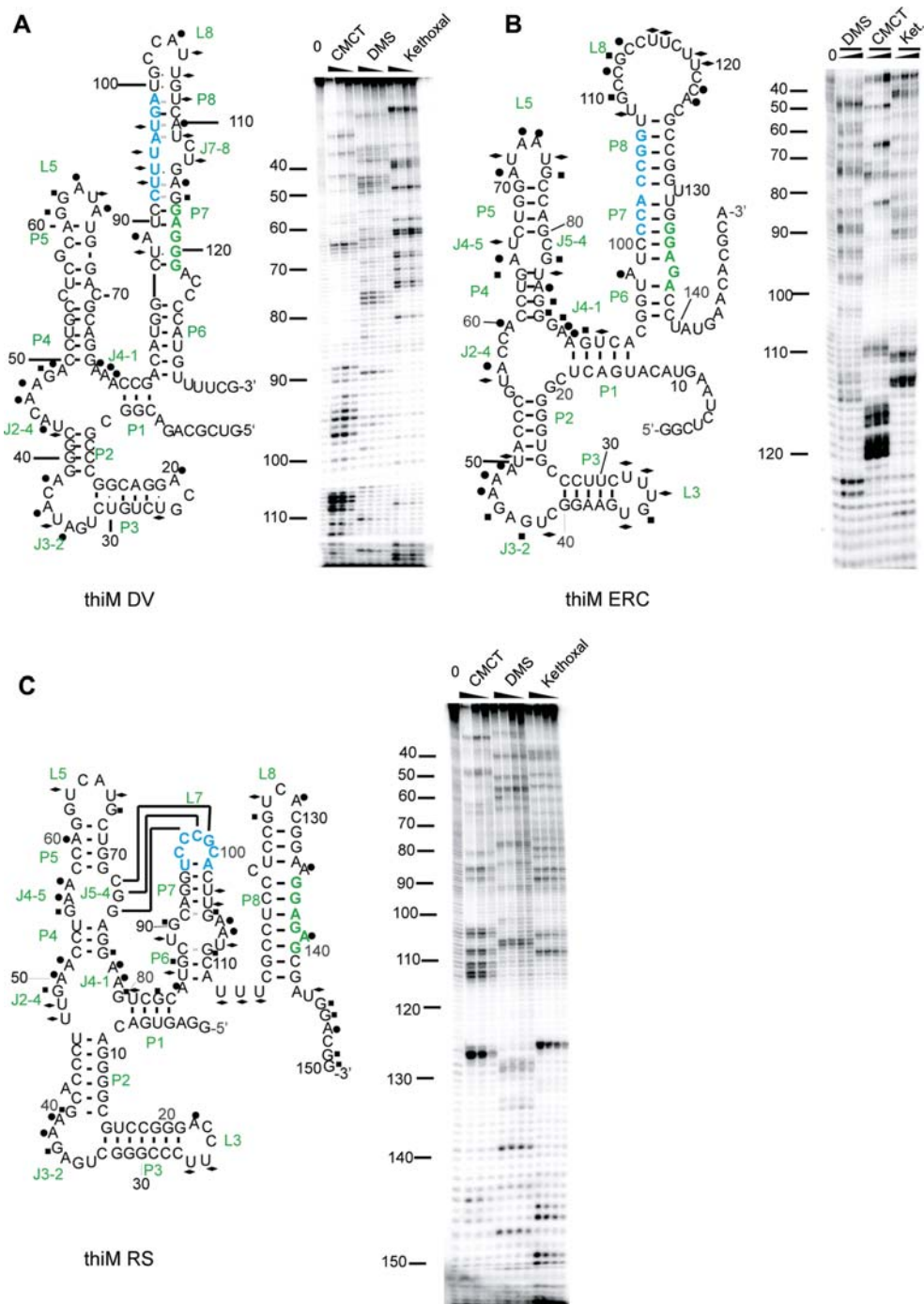


Figure 3 Secondary structure of full-length thiM riboswitches from *D. vulgaris*, *E. carotovora* and *R. spheroides*.

(A) Secondary structure of the full-length thiM riboswitch from *D. vulgaris* and primer extension reactions after chemical modifications of the riboswitch with 1-cyclohexyl-3-(2-morpholinoethyl)-carbodiimide (CMCT), dimethyl sulfate (DMS) and 2-keto-3-ethoxybutyraldehyde bis-thiosemicarbazone (kethoxal). Positions that are chemically modified are marked with symbols (DMS, black dot; kethoxal, black square; CMCT, black diamond). The concentrations of the probing agents in each lane were: kethoxal – 2.5 mM, 5 mM, 10 mM, 20 mM; DMS – 7.5 mM, 15 mM, 30 mM, 60 mM; CMCT – 5 mM, 20 mM, 50 mM (from right to left). Untreated RNA is referred to as 0. The Shine-Dalgarno sequence is shown in green. Nucleotides complementary to designed hairpins are highlighted in blue. (B) Secondary structure of the full-length thiM riboswitch from *E. carotovora* and primer extension reactions after chemical modifications of the riboswitch with CMCT, DMS and kethoxal. Positions are marked in the same way as in panel (A). (C) Secondary structure of the full-length thiM riboswitch from *R. spheroides* and primer extension reactions after chemical modifications of the riboswitch with CMCT, DMS and kethoxal. Positions are marked in the same way as in panel (A).

ively modifies single stranded Gs. As shown in Figure 3A, the selectivity of kethoxal for single-stranded Gs was weak at the highest concentration of the probe. At the highest concentration of kethoxal, almost all of the guanosine residues are modified. However, some of the gua-

nosine residues show only weak, if any, modification at the lower kethoxal concentrations, presumably because they are involved in Watson-Crick pairing. Alternatively, these purines might be involved in the formation of non-canonical double-stranded regions.

At the lowest concentrations of the probe, residues G48, G58 and G61/G62 are clearly modified by kethoxal. These data support the secondary structure shown in Figure 3A and strongly suggest that, e.g., the three consecutive G-residues G39–G42 are engaged in the formation of the fairly stable stem P2.

Chemical probing of thiM riboswitch from *E. carotovora* Chemical probing also confirmed the conserved secondary structure of the THI-element for the full-length ERC thiM riboswitch construct (Figure 3B). Modifications correspond to the single-stranded regions L3, J3-2, J2-4, J4-5, L5, J5-4 as well as J4-1. Stems P1 and P4 seem to be only loosely base paired as some modifications can be observed within the corresponding nucleotides. We have reason to believe that these stems are stabilized in the presence of TPP, because modifications of G90, U91 and G85 are decreased in the presence of TPP (data not shown). In ERC, the expression domain forms a large hairpin loop L8 adjacent to fairly stable stems P8, P7 and P6. Chemical probing clearly confirms the single stranded nature of the nucleotides within hairpin loop L8. Again, it was not possible to unambiguously resolve the SD sequence due to overlapping primer-binding sites.

Chemical probing of thiM riboswitch from *R. spheroides* Chemical probing of a full-length thiM riboswitch construct corresponding to RS also confirmed the secondary structure of the THI-element (Figure 3C). Stems P2, P3, P4 and P5 were not modified, whereas loops L3, L5 as well as bulges J3-2, J2-4, J4-5 and J4-1 were clearly modified, indicating single-stranded regions. Interestingly, no modifications could be found for bulge J5-4. The expression domain of RS shows little similarity to the previously analyzed expression domains and comprises two hairpin loops, rather than one hairpin. Here, we propose the formation of a hairpin loop L8 which shows the most intensive modifications for G126 and U127 and resides on a long stem P8, which is only disrupted by the bulged-out residues C122, A134 and A139. We also propose the formation of an unexpected hairpin loop L7 adjacent to stems P7 and possibly P6. However, the formation of stem P6 has to be further validated, because each base pair of this helix contains a nucleotide accessible to chemical modification. Stems P6 and P7 are connected by two junctions indicated by modifications for single-stranded G90 and U89 (J6-7), as well as single stranded G109, U108, A107, A106 (J7-6). Interestingly, the residues proposed to form the loop L7, however, do not become modified by chemical probing. This may be explained by the formation of a stable pseudoknot structure between J5-4 and L7 via base pairing of C72, G73, G74 of J5-4 with C97, C98 and G99 of L7.

In the case of RS, the SD sequence could be resolved by chemical probing, because our construct was longer than the one depicted in Figure 3C. However, only A139 was clearly modified in the absence of TPP. J6-8 consisting of three consecutive U-residues becomes strongly modified in chemical probing in accordance with a single-stranded region, as depicted in Figure 3C.

Design of RNA-hairpins based on *in vitro* selected hairpins for the *E. coli* riboswitch

We have previously identified short RNA hairpin motifs by *in vitro* selection, which tightly bound to parts of the expression domain from the thiM riboswitch from *E. coli*, in the absence of TPP, but not in its presence (Mayer et al., 2007). These hairpin motifs presumably recognized a stem-loop structure in the expression domain, which was complementary to their own loop sequence, by high-affinity kissing-loop interactions. Based on these findings, we designed analogous hairpin motifs for the thiM riboswitches from *D. vulgaris*, *E. carotovora* and *R. spheroides* and used them to analyze secondary structure changes within the expression domains of the respective riboswitches. Figure 4A shows the secondary structure of the three hairpin motifs. Nucleotides complementary to the expression domains of the respective riboswitches are represented in blue. Figure 3 shows the nucleotides in the respective riboswitches also in blue, which are complementary to the designed hairpins and therefore putative hairpin binding sites. Using filter-binding assays, we first confirmed binding of our designed hairpin constructs to their respective riboswitches (Figure 4B). The hairpin motifs bound with dissociation constants of 64 nM (DV), 3 nM (ERC) and 5 nM (RS), respectively, to their cognate riboswitches. No cross binding to other riboswitches was observed (data not shown). These affinities may reflect the number of G/C base pairs involved in the interaction. Interestingly, all hairpin motifs required the presence of Mg^{2+} ions for binding (5–20 mM). Without Mg^{2+} , no binding was detectable (data not shown).

We next tried to disrupt the hairpin-riboswitch interaction by TPP and thiamine, respectively, by inducing a structural rearrangement of the riboswitches (Figure 4C). Herein, TPP was able to compete with hairpin binding at low mM concentrations (black bars), whereas no competition was observed with thiamine (white bars). These results indicate that the sequence complementary to the loop region of the hairpin motifs becomes engaged in strong base-pairing interaction in the presence of TPP, as shown for the proposed secondary structures in the presence of TPP of *D. vulgaris* and *E. carotovora* (Figure 3A,B). Likewise, these data also support the notion that the base pairing of the SD sequence is also increased in the presence of TPP.

In the case of *R. spheroides*, the designed hairpin was complementary to our proposed loop L7, which we claim to be involved in formation of a pseudoknot with J5-4. Again, TPP but not thiamine competes with binding of the hairpin to the riboswitch. Thus, the hairpin loop L7 and adjacent stems P7 and P6 appear to be important structural motifs of the thiM riboswitch from *R. spheroides*.

Discussion

Phylogenetic comparisons with thiM riboswitches from other bacteria that function like the one in *E. coli* showed that despite significant differences in the expression domains of different organisms, remarkably similar

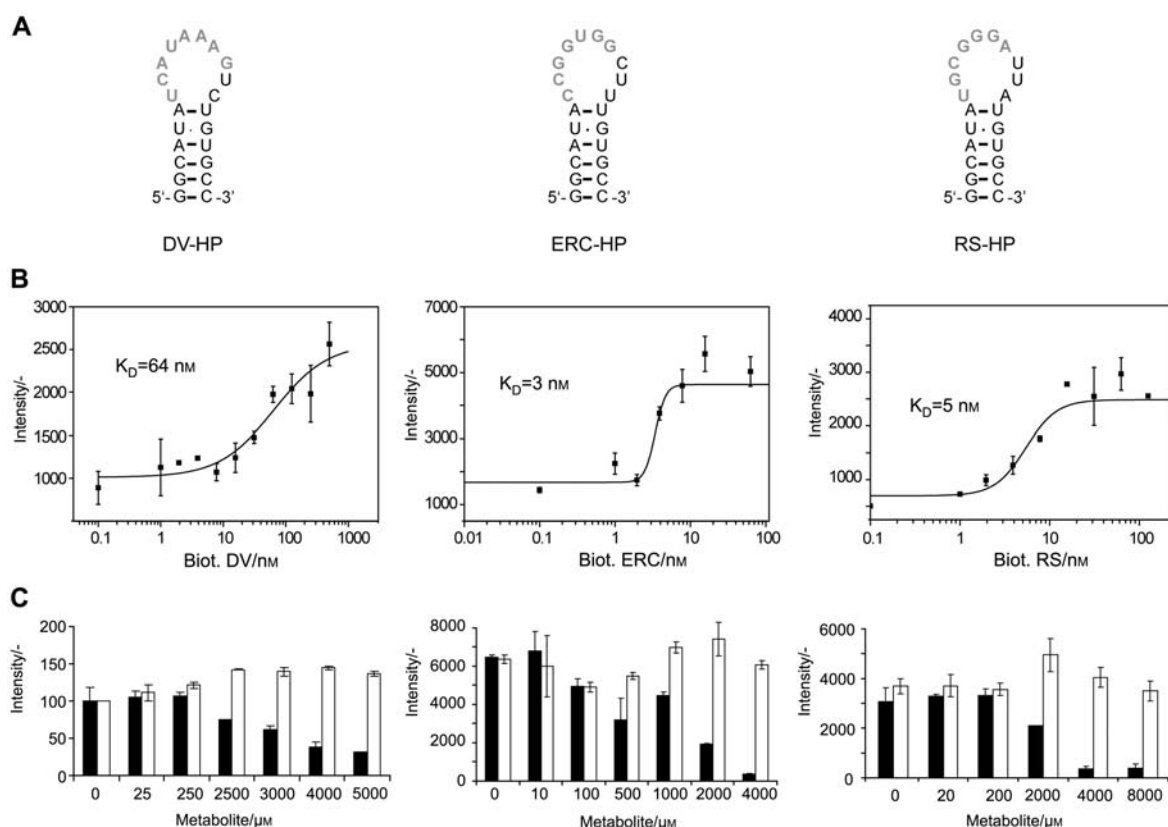


Figure 4 Hairpin-based analysis of secondary structure changes within the expression domains of riboswitches from *D. vulgaris*, *E. carotovora* and *R. spheroides*.

(A) Hairpins designed to bind to the expression domains of thiM riboswitches from *D. vulgaris* (DV-HP), *E. carotovora* (ERC-HP) and *R. spheroides* (RS-HP). Nucleotides complementary to the respective expression domain are shown in bold gray font. (B) Affinity determinations of hairpins binding to their respective expression domain. Dissociation constants of 64 nM (DV), 3 nM (ERC) and 5 nM (RS) were determined. (C) Metabolite-specific competition of designed hairpin motifs. The interaction of each RNA hairpin with the corresponding riboswitch can be specifically competed with TPP (black bars). No competition was observed with thiamine (white bars).

modes of interdomain recognition are utilized. In the three organisms analyzed here, TPP induces the folding of the expression domains into hairpin loops that trap accessibility of the SD sequence in long extended stems, similar to the thiM riboswitch from *E. coli*. The RNAs are localized in the 5'-UTR of the HET gene, lack a poly-U stretch in the 5'-vicinity of the SD sequence, and diverge in their aptamer domains by several mutations, whereas the expression domains show no similarities in their primary sequences.

Chemical probing of the DV thiM riboswitch confirmed a secondary structure related to the well-characterized thiM riboswitch from *E. coli*; the aptamer and expression domains seem to fold independently. The aptamer domain folds into a structure that is highly comparable to the secondary structure of the *E. coli* thiM aptamer domain. Stems P1–P5 are formed and provide a scaffold allowing conserved nucleotides to be exposed in single-stranded loop regions. The highly stable stem P2 consisting of three consecutive G/C base pairs is also present in all three riboswitches. Interestingly, in the least conserved riboswitch from DV, this stem is formed by C/G instead of G/C base pairs. The invariant ACCUG motif of the THI-element which is found within and adjacent to stem P4 was found to be entirely conserved in DV, ERC and RS. The two U-residues in loop L5 were

also found in ERC and RS. However, in DV there is only one U present in loop L5. The CGNAGG motif within J5-4 (CGN) and stem P4 (AGG) was conserved in all three riboswitches. Thus, stem P4 consists of entirely conserved nucleotides in all of the analyzed riboswitches. Also, a single stranded A nucleotide found by Rodionov et al. (2002) in the junction between P4 and P1 is conserved in all three riboswitches.

Remarkably, the TPP-binding domain in the thiM gene of *D. vulgaris* exhibits a similar affinity for TPP and discriminatory activity towards thiamine as does the structurally well-characterized riboswitch from *E. coli*, despite the considerable degree of variation between the two aptamer domains. This result indicates that even residues that contact the ligand directly can be substituted without significant alteration of the ligand-binding pocket in the RNA. However, one has to bear in mind that the second G within the UGAGA motif, which was mutated to a U in the case of *D. vulgaris*, participates only in stacking interactions with this ring and does not form hydrogen bonds with the HMP ring, as does the first G of the UGAGA motif. Therefore, the identity of the first G may be more important for the specific recognition of the HMP ring.

We have recently reported the *in vitro* selection of short RNA hairpins that bind to the thiM riboswitch of *E. coli*

in the absence of TPP and were specifically released upon addition of TPP (Mayer et al., 2007; Rentmeister et al., 2007). One of these hairpins was shown to interact with a defined loop region in the expression domain of the *E. coli* thiM riboswitch that existed only in the absence of the metabolite. Based on these previous findings, we designed short RNA hairpins that recognize their cognate riboswitch with high affinity and specificity, although the three riboswitches differed significantly in loop size and sequences. The interaction of the designed hairpins with their cognate riboswitches was efficiently competed by TPP, whereas addition of thiamine had no effect. The hairpins react on TPP-induced conformational changes within the expression domain, thus sensing the 'on' and 'off' states of the riboswitches. Binding of these small stem-loop motifs to their cognate riboswitches absolutely requires the presence of Mg^{2+} ions, providing strong evidence that this recognition depends on structural motifs, most likely interactions via kissing-loop complex formation, rather than mere sequence hybridization. Fluorescence-labeled versions of the TPP-released hairpins designed in this study might offer a strategy for the development of high-throughput screening assays based on fluorescence resonance energy transfer (FRET) or fluorescence polarization (Blount et al., 2006; Mayer and Famulok, 2006) to search for compounds that mimic TPP (Sudarsan et al., 2005). Such compounds might exhibit antibiotic or antifungal activity by selectively modulating riboswitches in pathogenic microorganisms, and might facilitate the establishment of riboswitches as a potential target class for new antimicrobial drugs.

Materials and methods

Oligonucleotides

DV-RS: 5'-GTC GCA GAC GGC GCC CGG CAG GAC GTC TGT CTG ATA CAG GGC TAC AAG ACC TGC CTC GCA GGA TAT GGA CGC AGG AAA CCG ACA TGG CTA TCC TTT ATG ATG CCA TTG TCA TCT GAG GAG GGA CCC CAT GTT TTC GAC A-3'; RS-RS template: 5'-GGA GTG ACA GGG GCG TCC GGG ACC TTC CCG GGC TGA GAA GCA CCC TTT GAA CCT GAA CCA GGT CAT GCT GGC GGA GGA AGT CGC ATG CTG CAG GTC CCG CAC TTG AAT GCA TTT CGC CTC CCT CCG TCA CGG AAG GAG AGC GAT GGA CGG CTG CGG AAC CTA TCT CCG ACA CCA TG-3'; ERC-RS template: 5'-GGC TCT AAG TAC ATG ACT CGG GGT GCC CTT CTT TGT GAA GGC TGA GAA ATA CCC GTA CCA CCT GAT CTG GAT AAT GCC AGC GTA GGG AAG TCA CGG TAT CCC ACC GGT TGC CGC CTT CTT CCA CGC CGG TTG GGA GAC CTA TGA ACA CGC A-3'.

Chemical probing of RNA secondary structures

Chemical probing was performed as described previously (Rentmeister et al., 2006, 2007). Modification with DMS or kethoxal: in a final volume of 10 μ l, RNA (0.2 μ g/ μ l) was incubated in 50 mM HEPES pH 7.8, 100 mM KCl and 10 mM $MgCl_2$ at 25°C for 30 min. Then, 1 μ l of a 600-mM solution of DMS in ethanol or 200 mM kethoxal (ICN, Eschwege, Germany) in water, respectively, was added, mixed and incubated for 20 min at 25°C. After precipitation, 5'-end labeled primer was annealed and primer extension performed. Modification with CMCT: in a final volume of 10 μ l, RNA (0.2 μ g/ μ l) was incubated in 50 mM potassium borate pH 8.0, 100 mM KCl and 10 mM $MgCl_2$ at 25°C for 30 min.

Then, 1 μ l of a 200-mM solution of CMCT in water was added, mixed and incubated for 20 min at 25°C. After precipitation, 5'-end labeled primer was annealed and primer extension performed. In a 20- μ l reaction, 0.2 μ g RNA in 50 mM Tris-HCl pH 8.3, 75 mM KCl, 3 mM $MgCl_2$, 20 mM DTT and 0.5 mM dNTPs (each) was heated to 65°C for 5 min, and then chilled on ice for 1 min. After addition of 1 μ l (200 U) of Superscript II Reverse Transcriptase (Invitrogen, Karlsruhe, Germany), the reaction was incubated at 42°C for 50 min, followed by inactivation at 70°C for 15 min. After precipitation, the DNA fragments were separated on an 8% denaturing PAA gel at 2000 V and visualized by phosphorimaging (FLA 3000, Fuji, Düsseldorf, Germany). The sequencing reactions were carried out using the PCR templates with the Sequenase Version 2.0 PCR Product Sequencing kit (USB, Cleveland, OH, USA).

Preparation of oligonucleotides

ThiM riboswitches were prepared from dsDNA templates, generated by PCR using the appropriate primers, by *in vitro* transcription and purified by PAGE. 5'-Biotinylated RNA was prepared by transcription in the presence of guanosine monophosphorothioate (GMPS), using 4-fold excess of GMPS over GTP, and subsequent treatment with iodoacetyl biotin (Pierce, Rockford, IL, USA) (Sengle et al., 2000). For the preparation of the RNA hairpins, the complementary oligonucleotides were hybridized and used for *in vitro* transcription by T7 RNA polymerase.

Filter-binding assays

To determine a K_d , 5'-[^{32}P]-labeled DV hairpin, ERC hairpin or RS hairpin were incubated with increasing amounts of the respective biotinylated RNA (0–500 nM) and 250 nM soluble streptavidin in binding buffer (10 mM HEPES pH 7.5, 100 mM KCl and 15 mM $MgCl_2$ for ERC and RS, 20 mM $MgCl_2$ for DV) for 30 min at room temperature. After incubation, the reactions were passed through a 0.45- μ m nitrocellulose membrane and washed four times with 200 μ l binding buffer. Bound RNA was quantified by phosphorimaging using advanced image data analysis (AIDA) to calculate intensities.

To quantify the efficiency by which TPP or thiamine, respectively, compete with the hairpins for RNA binding, we incubated biotinylated RNA (200 nM DV RNA, 10 nM ERC RNA, 20 nM RS RNA, respectively) with the 5'-[^{32}P]-labeled hairpins and increasing amounts of TPP (Sigma, St. Louis, MO, USA) or thiamine (Sigma) (0–5000 μ M), respectively, as described above. Both assays were performed in duplicates.

Isothermal titration calorimetry

DV RNA was dialyzed against buffer (10 mM HEPES pH 7.5, 100 mM KCl, 5 mM $MgCl_2$) at 4°C overnight. Following dialysis, the buffer was used to prepare a TPP or thiamine solution at a concentration that was approximately 7.5-fold higher than the RNA (typically around 8.5 μ M and 65 μ M, respectively). All experiments were performed with a CSC ITC instrument (Calorimetric Sciences/TA instruments, Eschborn, Germany) at 25°C by titrating 23–33 injections of 5 μ l TPP or thiamine, respectively, into the RNA sample. Data were analyzed using BindWorks ITC software (Calorimetric Sciences) and fit to a single-site binding model.

Acknowledgments

This work was supported by grants from the Deutsche Forschungsgemeinschaft. A.R. thanks the Austrian Academy of Sciences for a grant from the Doctoral Scholarship Program.

References

- Batey, R.T., Gilbert, S.D., and Montange, R.K. (2004). Structure of a natural guanine-responsive riboswitch complexed with the metabolite hypoxanthine. *Nature* **432**, 411–415.
- Blount, K., Puskarz, I., Penchovsky, R., and Breaker, R. (2006). Development and application of a high-throughput assay for glmS riboswitch activators. *RNA Biol.* **3**, 77–81.
- Borovok, I., Gorovitz, B., Schreiber, R., Aharonowitz, Y., and Cohen, G. (2006). Coenzyme B12 controls transcription of the streptomyces class Ia ribonucleotide reductase nrdABS operon via a riboswitch mechanism. *J. Bacteriol.* **188**, 2512–2520.
- Corbino, K.A., Barrick, J.E., Lim, J., Welz, R., Tucker, B.J., Puskarz, I., Mandal, M., Rudnick, N.D., and Breaker, R.R. (2005). Evidence for a second class of S-adenosylmethionine riboswitches and other regulatory RNA motifs in α -proteobacteria. *Genome Biol.* **6**, R70.
- Edwards, T.E. and Ferre-D'Amare, A.R. (2006). Crystal structures of the thi-box riboswitch bound to thiamine pyrophosphate analogs reveal adaptive RNA-small molecule recognition. *Structure* **14**, 1459–1468.
- Fuchs, R.T., Grundy, F.J., and Henkin, T.M. (2006). The S(MK) box is a new SAM-binding RNA for translational regulation of SAM synthetase. *Nat. Struct. Mol. Biol.* **13**, 226–233.
- Henkin, T.M. and Grundy, F.J. (2006). Sensing metabolic signals with nascent RNA transcripts: the T box and S box riboswitches as paradigms. *Cold Spring Harb. Symp. Quant. Biol.* **71**, 231–237.
- Kubodera, T., Watanabe, M., Yoshiuchi, K., Yamashita, N., Nishimura, A., Nakai, S., Gomi, K., and Hanamoto, H. (2003). Thiamine-regulated gene expression of *Aspergillus oryzae* thiA requires splicing of the intron containing a riboswitch-like domain in the 5'-UTR. *FEBS Lett.* **555**, 516–520.
- Mandal, M. and Breaker, R.R. (2004). Adenine riboswitches and gene activation by disruption of a transcription terminator. *Nat. Struct. Mol. Biol.* **11**, 29–35.
- Mandal, M., Lee, M., Barrick, J.E., Weinberg, Z., Emilsson, G.M., Ruzzo, W.L., and Breaker, R.R. (2004). A glycine-dependent riboswitch that uses cooperative binding to control gene expression. *Science* **306**, 275–279.
- Mayer, G. and Famulok, M. (2006). High-throughput-compatible assay for glmS riboswitch metabolite dependence. *ChemBioChem* **7**, 602–604.
- Mayer, G., Raddatz, M.S., Grunwald, J.D., and Famulok, M. (2007). RNA ligands that distinguish metabolite-induced conformations in the TPP riboswitch. *Angew. Chem. Int. Ed. Engl.* **46**, 557–560.
- Miranda-Rios, J. (2007). The THI-box riboswitch, or how RNA binds thiamin pyrophosphate. *Structure* **15**, 259–265.
- Miranda-Rios, J., Navarro, M., and Soberon, M. (2001). A conserved RNA structure (thi box) is involved in regulation of thiamin biosynthetic gene expression in bacteria. *Proc. Natl. Acad. Sci. USA* **98**, 9736–9741.
- Montange, R.K. and Batey, R.T. (2006). Structure of the S-adenosylmethionine riboswitch regulatory mRNA element. *Nature* **441**, 1172–1175.
- Nahvi, A., Barrick, J.E., and Breaker, R.R. (2004). Coenzyme B12 riboswitches are widespread genetic control elements in prokaryotes. *Nucleic Acids Res.* **32**, 143–150.
- Noeske, J., Richter, C., Grundl, M.A., Nasiri, H.R., Schwalbe, H., and Wöhnert, J. (2005). An intermolecular base triple as the basis of ligand specificity and affinity in the guanine- and adenine-sensing riboswitch RNAs. *Proc. Natl. Acad. Sci. USA* **102**, 1372–1377.
- Noeske, J., Richter, C., Stiraln, E., Schwalbe, H., and Wöhnert, J. (2006). Phosphate-group recognition by the aptamer domain of the thiamine pyrophosphate sensing riboswitch. *ChemBioChem* **7**, 1451–1456.
- Noeske, J., Buck, J., Furtig, B., Nasiri, H.R., Schwalbe, H., and Wöhnert, J. (2007). Interplay of 'induced fit' and preorganization in the ligand induced folding of the aptamer domain of the guanine binding riboswitch. *Nucleic Acids Res.* **35**, 572–583.
- Nudler, E. (2006). Flipping riboswitches. *Cell* **126**, 19–22.
- Rentmeister, A., Bill, A., Wahle, T., Walter, J., and Famulok, M. (2006). RNA aptamers selectively modulate protein recruitment to the cytoplasmic domain of β -secretase BACE1 *in vitro*. *RNA* **12**, 1650–1660.
- Rentmeister, A., Mayer, G., Kuhn, N., and Famulok, M. (2007). Conformational changes in the expression domain of the *Escherichia coli* thiM riboswitch. *Nucleic Acids Res.* **35**, 3713–3722.
- Rodionov, D.A., Vitreschak, A.G., Mironov, A.A., and Gelfand, M.S. (2002). Comparative genomics of thiamin biosynthesis in prokaryotes. New genes and regulatory mechanisms. *J. Biol. Chem.* **277**, 48949–48959.
- Sengle, G., Jenne, A., Arora, P.S., Seelig, B., Nowick, J.S., Jaschke, A., and Famulok, M. (2000). Synthesis, incorporation efficiency, and stability of disulfide bridged functional groups at RNA 5'-ends. *Bioorg. Med. Chem.* **8**, 1317–1329.
- Serganov, A., Yuan, Y.R., Pikovskaya, O., Polonskaia, A., Malinina, L., Phan, A.T., Hobartner, C., Micura, R., Breaker, R.R., and Patel, D.J. (2004). Structural basis for discriminative regulation of gene expression by adenine- and guanine-sensing mRNAs. *Chem. Biol.* **11**, 1729–1741.
- Serganov, A., Polonskaia, A., Phan, A.T., Breaker, R.R., and Patel, D.J. (2006). Structural basis for gene regulation by a thiamine pyrophosphate-sensing riboswitch. *Nature* **441**, 1167–1171.
- Sudarsan, N., Barrick, J.E., and Breaker, R.R. (2003a). Metabolite-binding RNA domains are present in the genes of eukaryotes. *RNA* **9**, 644–647.
- Sudarsan, N., Wickiser, J.K., Nakamura, S., Ebert, M.S., and Breaker, R.R. (2003b). An mRNA structure in bacteria that controls gene expression by binding lysine. *Genes Dev.* **17**, 2688–2697.
- Sudarsan, N., Cohen-Chalamish, S., Nakamura, S., Emilsson, G.M., and Breaker, R.R. (2005). Thiamine pyrophosphate riboswitches are targets for the antimicrobial compound pyri-thiamine. *Chem. Biol.* **12**, 1325–1335.
- Sudarsan, N., Hammond, M.C., Block, K.F., Welz, R., Barrick, J.E., Roth, A., and Breaker, R.R. (2006). Tandem riboswitch architectures exhibit complex gene control functions. *Science* **314**, 300–304.
- Thore, S., Leibundgut, M., and Ban, N. (2006). Structure of the eukaryotic thiamine pyrophosphate riboswitch with its regulatory ligand. *Science* **312**, 1208–1211.
- Winkler, W.C. and Breaker, R.R. (2003). Genetic control by metabolite-binding riboswitches. *ChemBioChem* **4**, 1024–1032.
- Winkler, W.C. and Breaker, R.R. (2005). Regulation of bacterial gene expression by riboswitches. *Annu. Rev. Microbiol.* **59**, 487–517.
- Winkler, W., Nahvi, A., and Breaker, R.R. (2002). Thiamine derivatives bind messenger RNAs directly to regulate bacterial gene expression. *Nature* **419**, 952–956.
- Winkler, W.C., Nahvi, A., Sudarsan, N., Barrick, J.E., and Breaker, R.R. (2003). An mRNA structure that controls gene expression by binding S-adenosylmethionine. *Nat. Struct. Mol. Biol.* **10**, 701–707.
- Winkler, W.C., Nahvi, A., Roth, A., Collins, J.A., and Breaker, R.R. (2004). Control of gene expression by a natural metabolite-responsive ribozyme. *Nature* **428**, 281–286.
- Yamauchi, T., Miyoshi, D., Kubodera, T., Nishimura, A., Nakai, S., and Sugimoto, N. (2005). Roles of Mg²⁺ in TPP-dependent riboswitch. *FEBS Lett.* **579**, 2583–2588.